

## Effect of Hydrothermal Growth Temperature and Time on Physical Properties And Photoanode Performance of ZnO Nanorods

Asla. A. AL-Zahrani<sup>1,2</sup>, Zulkarnain Zainal<sup>1,3\*</sup>, Zainal Abidin Talib<sup>4</sup>, Janet Lim Hong Ngee<sup>1,3</sup>, Laimy Mohd Fudzi<sup>1</sup>, Araa Mebdir Holi<sup>5</sup> and Mahanim Sarif @Mohd Ali<sup>1,6</sup>

<sup>1</sup>Department of Chemistry, Faculty of Science, Universiti Putra Malaysia, 43400 UPM Serdang, Selangor, Malaysia.

<sup>2</sup>Imam Abdulrahman bin Fiasal University, eastern region, Dammam, Saudi Arabia.

<sup>3</sup>Materials Synthesis and Characterization Laboratory, Institute of Advanced Technology, Universiti Putra Malaysia, 43400 UPM Serdang, Selangor, Malaysia.

<sup>4</sup>Department of Physics, Faculty of Science, Universiti Putra Malaysia, 43400 UPM Serdang, Selangor, Malaysia.

<sup>5</sup>Department of Physics, College of Education, University of Al-Qadisiyah, Al-Diwaniyah, Al-Qadisiyah 58002, Iraq.

<sup>6</sup>Forest product Division, Forest Research Institute Malaysia, 52109 Kepong, Selangor, Malaysia.

Received 18 September 2019, Revised 6 March 2020, Accepted 12 March 2020

### ABSTRACT

Well aligned zinc oxide (ZnO) nanorods (NRs) on ITO substrate for photoelectrochemical application were synthesized successfully through two steps preparation which consisted of deposition ZnO NPs by sol-gel spin coating at 3000 rpm for 40 sec. then followed by cost-effective simple hydrothermal method. The study investigates the effect of growth temperature and duration on the optical properties, photoconversion efficiency, and morphological structure of ZnO/ITO NRs. The hydrothermal temperature was varied between 80 °C to 120 °C and the growth time between 1 to 5 hours. The results of X-ray diffraction showed that the samples had a single hexagonal phase with a strong (002) preferred orientation. ZnO NRs prepared at 110 °C showed the highest diffraction peak intensity with crystallite size of 30.07 nm which implies the excellent crystallinity obtained at this temperature. FE-SEM proved that the temperature and growth time critically affect the diameter and the length of NRs. Photocurrent density of 0.337 mA/cm<sup>2</sup> at +0.5 V vs Ag/AgCl reference electrode shown by ZnO NRs photoelectrode prepared at 110 °C for 4 hours which is about 8 times greater than ZnO nanoparticles.

**Keywords:** Hydrothermal Method, Hydrothermal Growth Temperature, Growth Time, ZnO Nanorods.

### 1. INTRODUCTION

Nanocrystalline materials electrodes have opened a new era in the field of photoelectrochemical cells (PECs) application since material properties change depending on the size of the crystal and the thickness of the thin film. PEC performance is effectively determined through quantum size effects, which is beneficial to change the electric and light absorption properties. The ability of harvesting visible light, architectural structure, charge carrier transportation, and properties of photoanode material like charge carrier separation determines the PEC efficiency. Semiconductor materials are considered as one of the most important materials that can be used in PEC, effectively. Among diverse semiconductors based on metal oxide such as TiO<sub>2</sub> [1], Fe<sub>2</sub>O<sub>3</sub> [2], ZnO [3]-[5], and WO<sub>3</sub> [6]; a relatively large bandgap of about 3.3 to 3.4 eV is possessed by ZnO. The presence of large bandgap increases superiority of ZnO as it has high breakdown voltage, large electric field conditions, good stability at high temperature, and decreased

electronic noise [7]. ZnO possesses a 10 to 100-fold higher electron mobility leading to higher electron transmission efficiency, as compared to TiO<sub>2</sub> [8]. Moreover, the attractiveness of ZnO for many optoelectronic applications is signified through the presence of exciton binding energy of ZnO is 60 meV at 300 °K [9,10]. Owing to the quantum confinement effect, nanostructured ZnO usually exhibits enhanced optical properties, which have been intensively applied in photonic or photoelectrical devices [7]. The field of nanotechnology is fascinated with the optical, structural, and electrical properties of ZnO.

A variety of preparation approaches have been industrialized for synthesizing 1D-ZnO nanostructures. The seeded methods like electrochemical deposition and hydrothermal method [11] or seedless method like van der Waals epitaxy [7] can synthesize ZnO NRs as arrayed thin films on planar substrates. This synthesis authorizes successful deposition of ZnO NRs arrays on a variety of substrates, like metals, graphene, and transparent conductive oxides. A well-aligned ZnO NRs can be synthesized by physical evaporation [12], radio frequency [13], magnetron sputtering [14], electrophoretic deposition [15], and hydrothermal method [16, 17, 18]. Despite the positive aspects, severe experimental circumstances like precise gas, high temperature, and controlling gas flow rate are also required. Therefore, it is crucial to find simple and a low-temperature method to match the needs of high performance of PECs without sophisticated equipment and control of the growth parameters.

The present study has selected the hydrothermal method since it has become an attractive method due to many advantages, including low cost, no requirements of complicated instrumentation, and acceptability of deposition different materials on various substrates. These advantages are appropriately emerged for deposition in large scale area to modify thin-film properties by adjusting and controlling the deposition experimental circumstances parameters [8]. Moreover, it can yield good quality thin films because of the slow growth processes, which facilitate better orientation of crystallites with grain structure improvement and configuration growth [19]. Alteration in hydrothermal parameters such as hydrothermal temperature and growth time lead to different length and diameter of ZnO NRs, which change the morphological properties, crystalline quality, bandgap energy, and photoconversion efficiency of PECs. Therefore, this study aims to grow ZnO NRs arrays with perpendicular alignment using a simple hydrothermal method by controlling the preparative parameters. These parameters include growth duration and temperature for improving the photoconversion efficiency of the PECs.

## **2. MATERIAL AND METHODS**

### **2.1 Substrate Cleaning**

The hydrothermal approach was used to grow ZnO NRs arrays on indium tin oxide glass (ITO). The substrate was cleaned before coating, as some contaminants might be present in ITO glass. The ITO with dimension (1.5 × 2.5 cm) substrates were cleaned ultrasonically using acetone and 2-propanol (IPA) for 15 minutes each. Afterwards, it was rinsed by deionized water (DI-H<sub>2</sub>O) (18.2 MΩ cm) to remove the solvent residues and the cleaned substrates were kept at room temperature for drying.

### **2.2 Preparation ZnO NPs Seed Layers via The Spin Coating Method**

Analytical grading was performed for all the chemical reagents of the study without any further purification. Sol-gel spin coating technique was used for preparing ZnO thin films on ITO substrates. Whereas, diethanolamine (DEA) and zinc acetate dihydrate (Zn(CH<sub>3</sub>COO)<sub>2</sub>·2H<sub>2</sub>O) were the initial solutions used in the synthesis procedure. DEA worked as a stabilizer; whereas, (Zn(CH<sub>3</sub>COO)<sub>2</sub>·2H<sub>2</sub>O) was used as a solvent for the preparation of precursor preparation. 10 ml

ethanol was used to liquify zinc acetate dihydrate and later of DEA was added at room temperature. The molarity of zinc acetate dihydrate and DEA was 0.1 M while the molar ratio of ethanol to zinc acetate dihydrate was 1:1. Colourless homogenized solution was obtained by stirring the solution at 60 °C for 30 minutes to obtain a colourless homogenized solution cooled down to room temperature and was left for ageing overnight to make it more glutinous [20].

At room temperature, the solution coated onto the pre-cleaned (ITO) substrate using spin coater (Midas System, SPIN-1200D) at 3000 rpm for 40 seconds. After this, a hot plate (Hot Plate Stirrer Digital Advanced, STERIPLAN, DURAN) was used to vaporize the residual solvent to dry the films by soft baking at 100 °C for 15 minutes. The practicable thickness of three layers of the film was acquired by repeating the process of deposition to drying three cycles. Tubular furnace (CARBOLITE) was used to strengthen multilayer films at 350 °C for one hour with a heating rate of 2 °C per min in the atmosphere. This served as the nucleation sites that allowed vertical growth of ZnO NRs at different growth temperatures and times.

### 2.3 Preparation vertically aligned ZnO NRs Arrays via Hydrothermal Method

Equimolar of zinc nitrate  $Zn(NO_3)_2 \cdot 6H_2O$  and hexamethylenetetramine (HMTA,  $C_6H_{12}N_4$ ) were used as the hydrothermal growth solution (nutrient solution) at concentration 0.04 M and the pH value 6.5. The side of coated ZnO seed layers on ITO substrate was loaded in sealable glass vials that contained 20 ml of the prepared growth aqueous solution facing the wall. Then, It was loaded into a pre-heated silicon oil bath at different growth temperatures: 80 °C, 90 °C, 100 °C, 110 °C, and 120 °C for 4 hours to optimize the growth temperature. Afterwards, the growth time was varied from 1 hour to 5 hours, respectively for the optimum sample (110 °C). There was no revitalization of growth solution during the hydrothermal process. The obtained ZnO NRs were washed continuously using (DI  $H_2O$ ) for the removal of amino complexes, ZnO NRs accumulation caused by water surface tension, and residual precursors [21].

## 3. RESULTS AND DISCUSSION

### 3.1 Effect of Growth Temperature on ZnO NRs

X-ray diffraction (Philipps PM1730 diffractometer (Panalytical X'Pert Pro MPD diffractometer) using  $Cu-K\alpha$  ( $\lambda=1.54 \text{ \AA}$ ) radiation at 40 kV and 40 Ma was used to investigate the crystallinity and purity of ZnO NRs arrays as a function of hydrothermal temperature and growth time. With scanning speed of  $5^\circ \text{ min}^{-1}$  at the range  $20^\circ < \theta < 80^\circ$ , the panalytical Xpert Highscore software and the scanning range was maintained within  $20^\circ$ - $80^\circ$ . X-ray diffractograms of ZnO NRs arrays prepared at different growth temperatures (80, 90, 100, 110, and 120 °C) are shown in Figure 1. The diffraction along with (100), (002), (101), (110), (103), and (112) planes of ZnO NRs attribute the diffraction peaks located at  $2\theta$  of  $31.77^\circ$ ,  $34.65^\circ$ ,  $36.25^\circ$ ,  $56.60^\circ$ ,  $62.86^\circ$ , and  $67.96^\circ$ , respectively.

The formation of ZnO NRs hexagonal wurtzite structure with (002) direction at a right angle to the ITO substrate was indicated through recorded diffraction peaks matched with (JCPDS file No. 00-0030888) and previous studies [17, 20]. ZnO usually grows along with the (002) orientation because of the lowered surface free energy of the plane [22]. Moreover, the diffraction patterns at  $30.53^\circ$  fit to diffraction from (222) plane of the underlying ITO substrate. It has been noticed that no peaks are matching to impurities, which were distinguished at the high purity of the resultant thin films. The average crystal sizes (D) were calculated using the Debye-Scherrer equation as below [19].

$$D = \frac{K\lambda}{\beta \cos\theta} \quad (1)$$

where;

- D = average crystal size  
 $\theta$  = Bragg diffraction angle  
 $\lambda$  = X-ray radiation wavelength 1.5405 Å  
 $\beta$  = Full width at half maximum [FWHM] value

The XRD peak position, FWHM and crystal size of ZnO NRs as a function of growth time are summarized in Table 1.

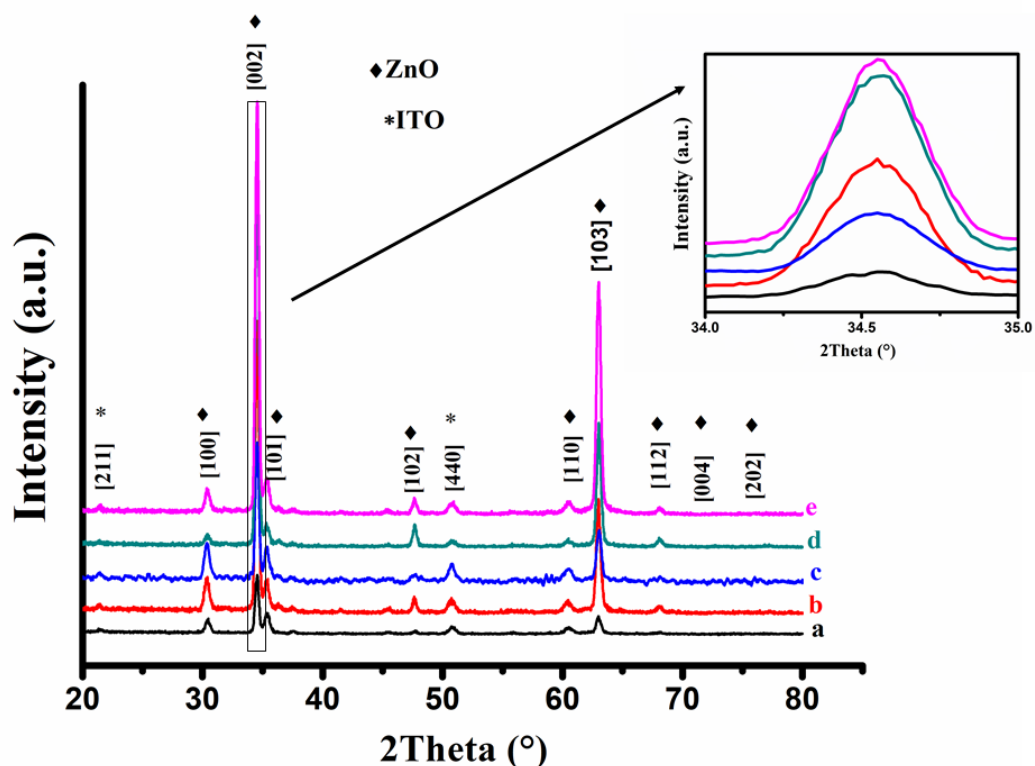


**Figure 1.** X-ray diffraction of ZnO NRs/ITO growth at different hydrothermal temperatures for 4 hours where (a) 80 °C; (b) 90 °C; (c) 100 °C; (d) 110 °C and (e) 120 °C. The inset of Figure 1 represents the (002) peak plotted from 34° to 35.5°.

**Table 1** Summarized data depicting the XRD patterns of aligned ZnO NRs/ITO

Temperature (°C)	2Theta (deg.)	FWHM (deg.)	Crystal size (nm)
80	34.5387	0.312	27.80
90	34.546	0.306	28.38
100	34.555	0.301	28.92
110	34.554	0.289	30.07
120	34.554	0.293	29.68

The relative intensities of the Bragg peaks in ZnO NRs patterns are consistent with strong orientation effects. The enhancement crystallinity properties of ZnO NRs were proved by XRD pattern as the hydrothermal temperature increases from 80 °C to 110 °C. However, decrement in the intensity of the dominant (002) plane was shown at 120 °C. The high intensity and narrow FWHM of a diffraction peak at (002) of the sample prepared at 110 °C implies the high improvement in the crystallinity of ZnO NRs at this temperature. The significant decrease of the intensity of the dominant (002) plane at 120 °C was mainly due to decrement concentration of Zn<sup>2+</sup> ions in pioneer solution, which leads to inhibition of the growing process of the nanorods [17]. FE-SEM help to investigate remarkable changes in the morphological structure of ZnO NRs as a function of growth temperature (Figure 2). Similarly, the corresponding cross-sectional view (inset) and top view surface micrographs were exhibited as a function of growth temperature. Figure 2 clarifies that all obtained samples showed rod-shaped with distinct hexagonal wurtzite structure. The rods were also observed to be standing vertically to the ITO substrates and there was still obvious porosity between them based on cross-sectional images of the samples. However, although, ZnO NRAs were formed at low temperature (80 °C), they were randomly oriented with relatively high density and they were not vertically aligned. Uniform formation of ZnO NRs occurred when hydrothermal temperature increased with increased length, density and distribution. The length and diameter were measured exploiting cross-sectional FE-SEM images by using Image software. The diameter and length of the rods were determined by measuring multiple rods in various locations and averaging their overall size.

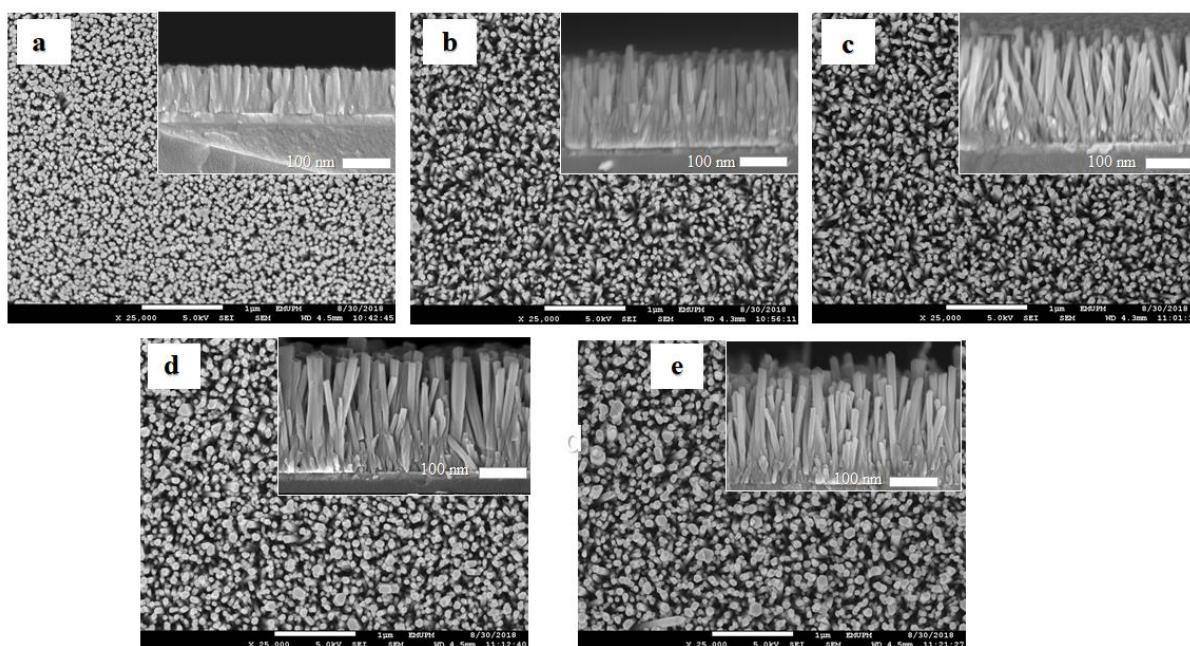


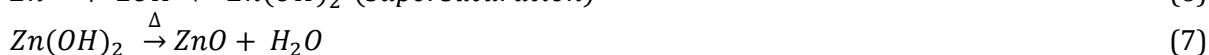
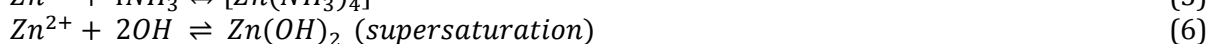
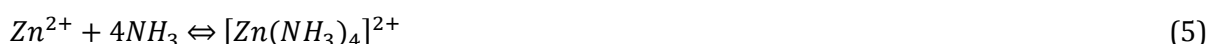
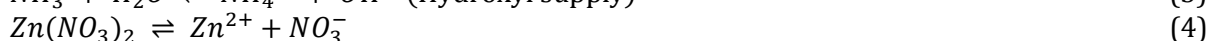
**Figure 2.** Top view and cross section FE-SEM images of ZnO NRs/ITO grown for 4 hours at different hydrothermal temperatures: (a) 80 °C; (b) 90 °C; (c) 100 °C; (d) 110 °C; and (e) 120 °C.

The perpendicular growth rate was determined in terms of length and diameter. The present study found that the length of the ZnO NRs increased significantly when the hydrothermal temperature increased from 80 °C to 110 °C. Afterwards, the thickness of rods was downturned, when the hydrothermal process was carried out at 120 °C due to the high growth rate at this temperature resulting in the rapid consumption of growth solution ions. The obtained FE-SEM images were consistent with XRD results. The thickness, diameter, and aspect ratio of ZnO NRs as a function of growth time are summarized in Table 2

**Table 2** Summarized data of the FE-SEM images (thickness, diameter, and aspect ratio),  $E_g$  values, and photocurrent density of aligned ZnO NRs/ITO

Temperature (°C)	Average length (nm)	Average diameter (nm)	Aspect ratio	$E_g$ (eV)	$J_{ph}$ (mA/cm <sup>2</sup> )
80	279.28	34.06	8.199	3.281	0.1228
90	556.74	34.51	16.13	3.277	0.1402
100	638.13	36.79	17.34	3.242	0.1920
110	758.59	37.10	20.45	3.234	0.3370
120	693.00	40.57	17.08	3.216	0.2276

The results showed that controlling growth temperature is considered an important parameter in obtaining the morphological structure with good distribution, well orientation alignment, density, length, and diameter that can match the requirements of PECs. The comparison between lateral and perpendicular growth presents the growth mechanism of ZnO NRs [8, 23]. From this aspect, it can be noticed that there was a constant increase in diameter and length simultaneously by increasing the temperature from 80 °C to 110°C. However, conducting the hydrothermal process at 120 °C resulted in decreased length of ZnO NRs and drastic increase in its diameter (Figure 3). There is a difference in surface energy for each crystal plane of ZnO due to increased consumption of  $Zn^{2+}$  and  $OH^-$ , therefore, ZnO NRs preferred growth laterally than vertically [8]. This finding implies that increasing hydrothermal temperature up 110 °C may inhibit the perpendicular growth and enhance the lateral growth. Following mechanism is applicable for hydrothermal growth of ZnO nanorods arrays using zinc nitrate  $Zn(NO_3)_2 \cdot 6H_2O$  and HMTA [7, 24, 25].



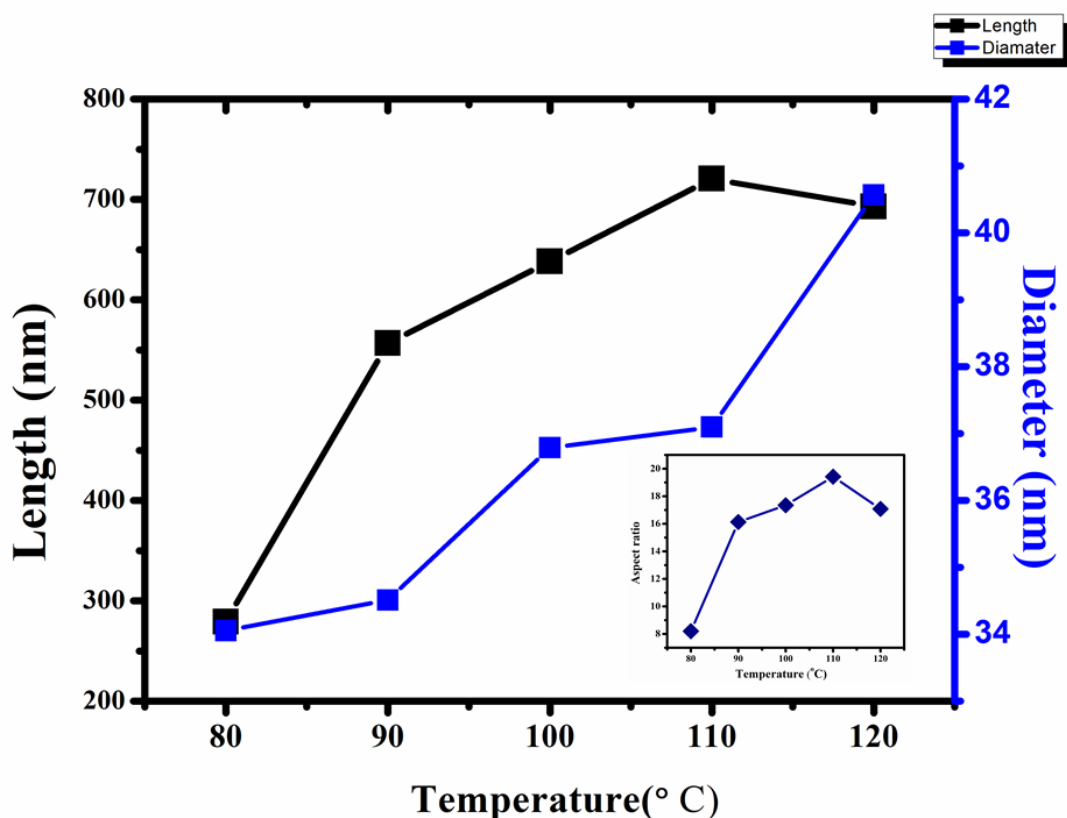


**Figure 3.** ZnO NRs growth temperature vs. change in length, diameter, and aspect ratio (inset).

There is a constant generation of  $Zn(OH)_2$  following continuous growth ZnO NRs depending on the continuous supply of  $Zn^{2+}$  ions from Zinc nitrate and  $OH^-$  ions from HMTA. This procedure is carried on until it reaches supersaturation stage, which finally converts to ZnO crystallite, grown along with c-axis orientation as ZnO NRs. These results are consistent with the XRD finding. Therefore, change in the hydrothermal temperature need to be controlled for obtaining the desired ZnO NRs and the feasible temperature at 110 °C.

UV-Vis spectrophotometer was used to investigate the optical properties of ZnO NRs grown on ITO at different hydrothermal temperatures ranging from 80 °C – 120 °C. The plotting of absorbance spectra are illustrated in Figure 4. The absorption edges of samples were found at 378.05, 379.20, 383.90, 385.09, and 393.65 nm of wavelengths for the ZnO NRs fabricated at 80°C, 90°C, 100°C, 110°C, and 120 °C, respectively. The absorption edge shifted towards longer wavelength (red-shift) as there is an increase in the growth temperature. The shift to a higher wavelength of the absorption edge caused by reducing the transition distance between energy levels known as bandgap energy [25].

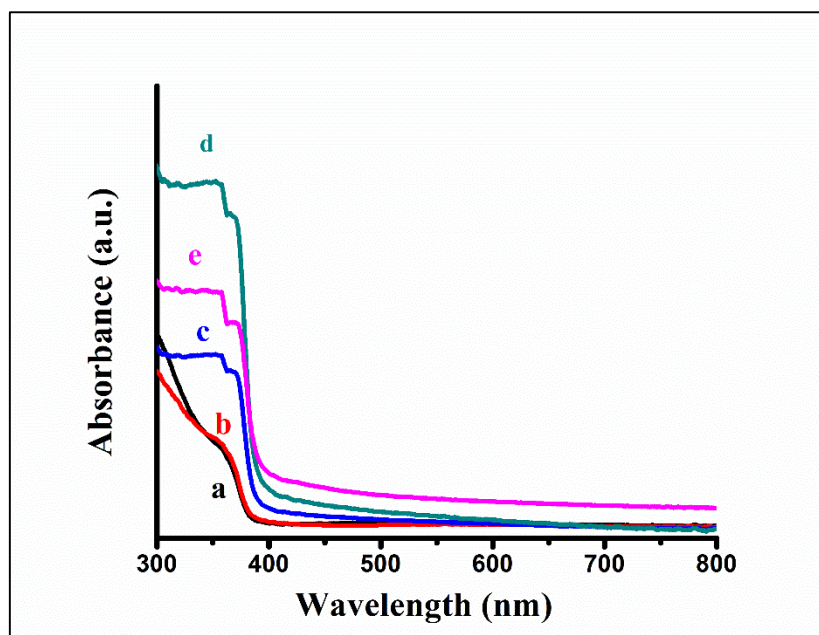


**Figure 4.** The absorbance spectra of ZnO NRs/ITO grown for 4 hours at different hydrothermal temperatures: (a) 80 °C; (b) 90 °C; (c) 100 °C; (d) 110 °C and (e) 120 °C.

The extrapolation of the linear portion of  $(\alpha hv)^2$  versus  $(hv)$  plot using Tauc Equation estimated the optical band gap energy of ZnO NRs synthesized via hydrothermal method as a function of growth temperature ranging between 80 °C and 120 °C [26].

$$(\alpha hv)^2 = A(hv - E_g)^n \quad (8)$$

Where,

$\alpha$  = absorption coefficient

$hv$  = energy of incident photon

A = constant

$E_g$  = optical band gap energy (eV)

$n$  = type of transmission (=  $\frac{1}{2}$  and 2 for allowed direct and indirect transmission respectively)

$n = \frac{1}{2}$  because ZnO is considered as direct transition [27-29]

Tauc plot of ZnO NRs fabricated by hydrothermal method considering growth temperature in the range between 80 °C and 120 °C is displayed in Figure 5; whereas, Table 2 listed the  $E_g$  values. The results obtained for optical band gap energy of ZnO NRs were in agreement with the previous studies [17, 20, 26,30], corresponding to direct transition band between the edges of valance band and conduction band. It is observed that the bandgap energy ( $E_g$ ) became narrower by increasing the hydrothermal temperature from 80 °C to 120 °C. This happened due to the increase of the crystal size caused by quantum size effect and the reduction of defects in ZnO NRs thin films with an increase in the hydrothermal temperature proven by XRD results.

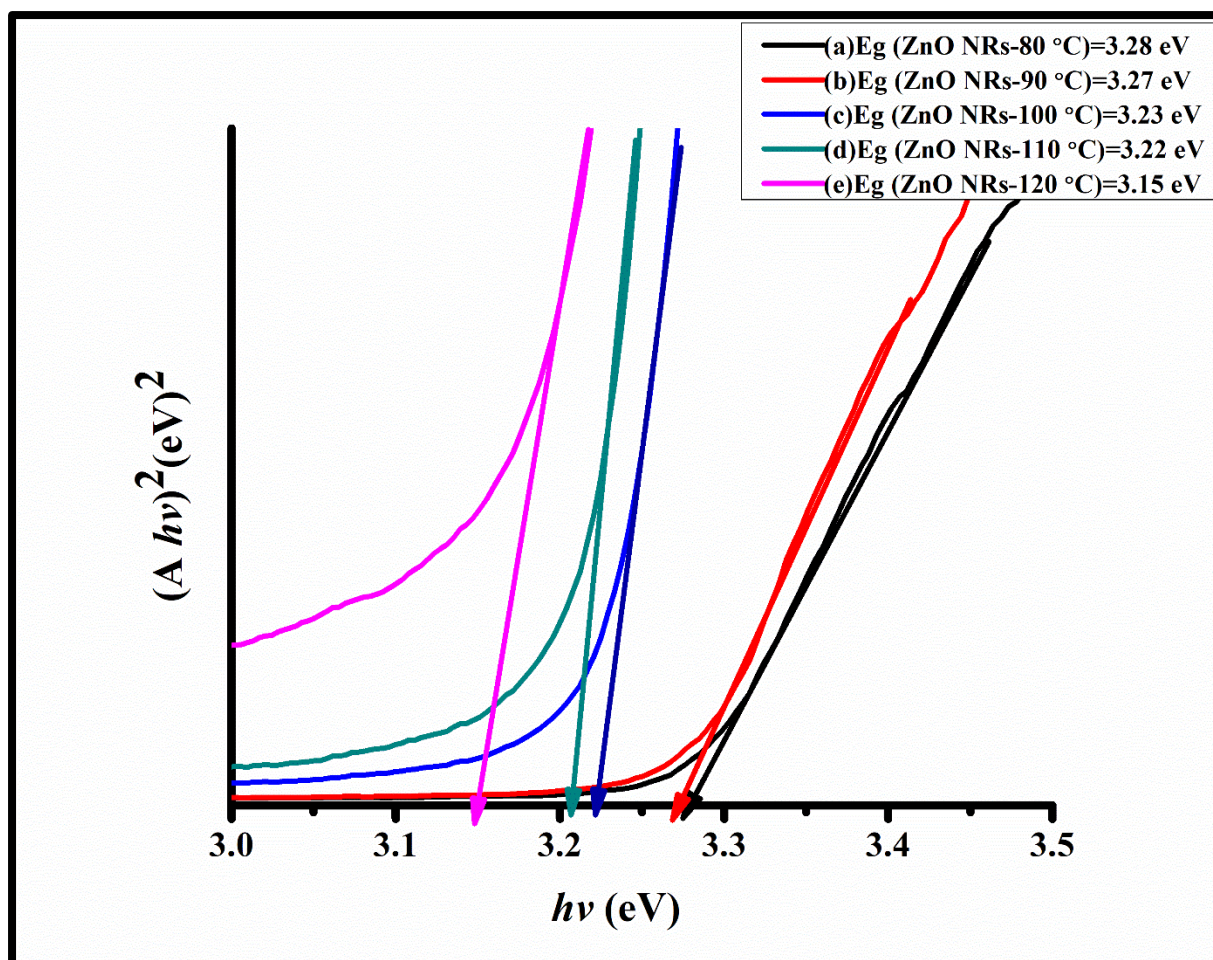


**Figure 5.** The Tauc plot  $(\alpha hv)^2$  versus energy  $(hv)$  of ZnO NRs/ITO grown for 4 hours at different hydrothermal temperatures: (a) 80 °C; (b) 90 °C; (c) 100 °C; (d) 110 °C and (e) 120 °C.

PEC performance based on ZnO NRs as a function of growth temperature ranging between 80 °C and 120 °C was evaluated using the three-electrodes electrochemical set up conducted under dark and stimulate radiation in an equimolar solution of 0.1M of  $\text{Na}_2\text{S}$  and  $\text{Na}_2\text{SO}_3$ . Figure 6 illustrates the PEC property of ZnO NRs/ITO photoanode electrode equipped through a simple hydrothermal method with a fixed growth time of 4 hours. The values of photocurrent density calculated at +0.5 V versus  $V_{\text{Ag}/\text{AgCl}}$  calculated through the linear sweep voltammetry collected from -0.5  $V_{\text{Ag}/\text{AgCl}}$  to +1  $V_{\text{Ag}/\text{AgCl}}$  of ZnO NRs photoanode with and without solar simulated radiation are summarized in Table 2. The results showed that increase in hydrothermal temperature from 80 °C to 110 °C enhanced the photocurrent density from 0.1228  $\text{mA}/\text{cm}^2$  to 0.3370  $\text{mA}/\text{cm}^2$  at the external potential applied of +0.5  $V_{\text{Ag}/\text{AgCl}}$  by ~76%. Controversially, the photocurrent density decreased afterwards by ~33% when the hydrothermal process was carried out at 120 °C (Figure 7). Reducing the working electrode surface area based on the aspect ratio results (Table 2) has suppressed the photocurrent density. Therefore, the photocurrent density of PEC decreased due to reduction in the aspect ratio of ZnO NRs at 120 °C based on XRD and FE-SEM results as earlier clarified.

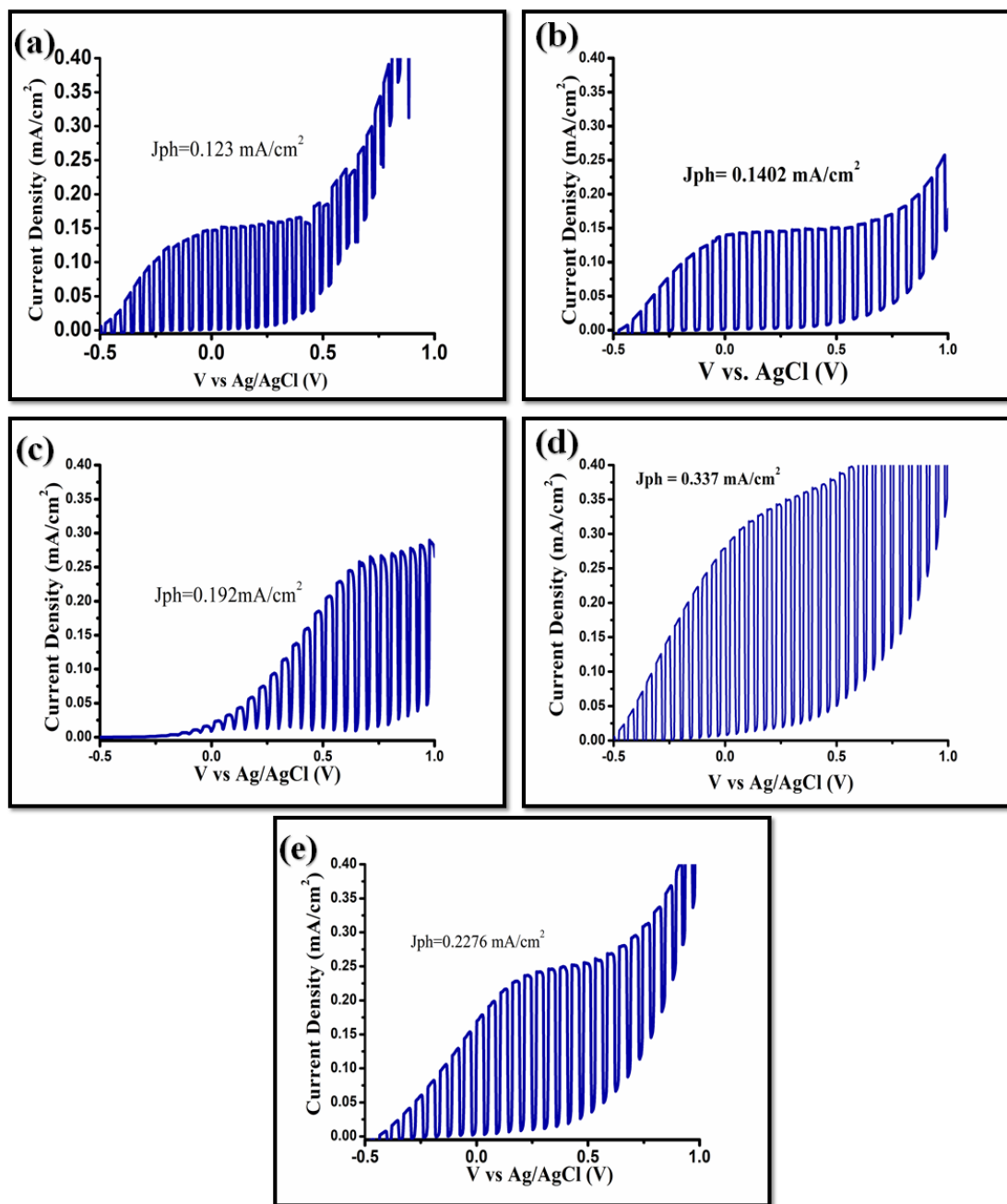


**Figure 6.** Linear sweep voltammograms of ZnO NRs/ITO synthesized at different hydrothermal temperatures for 4hours (a) 80 °C; (b) 90 °C; (c) 100 °C; (d) 110 °C and (e) 120 °C.

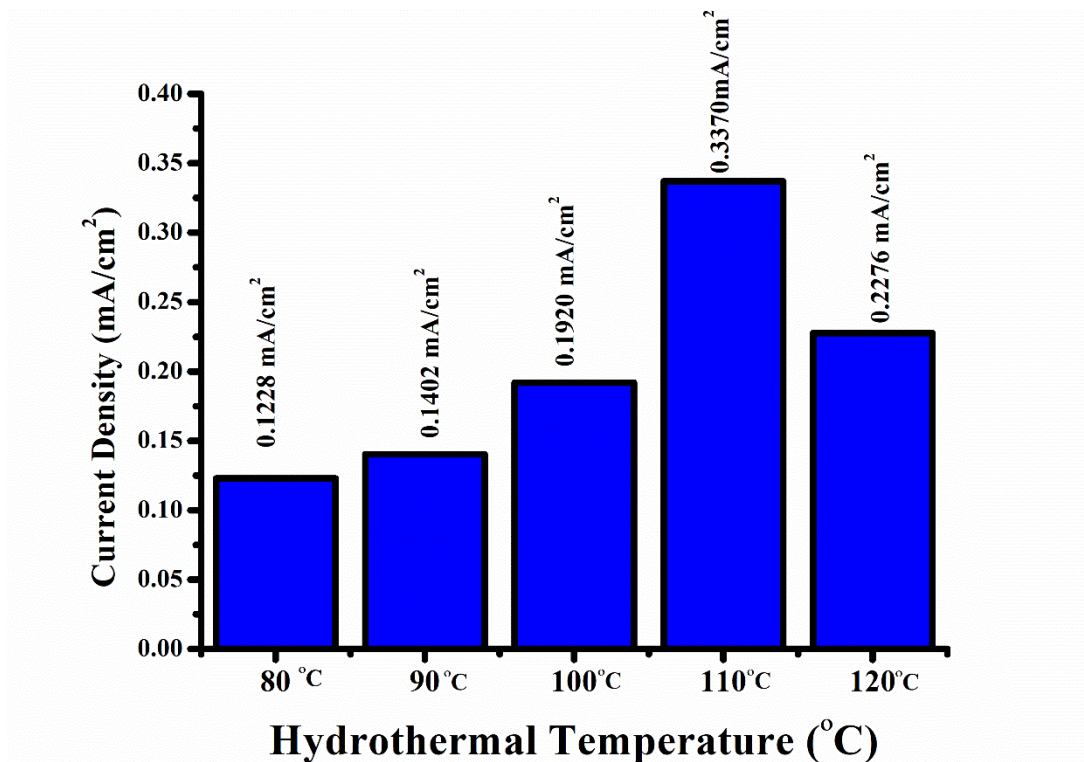


**Figure 7.** Photocurrent density  $J_{ph}$  (mA/cm<sup>2</sup>) plotted against growth temperature (°C) at applied potential of +0.5V.

### 3.2 Studying the Effect of Growth Time on ZnO NRs at 110 °C

The present study has thoroughly investigated the influence of hydrothermal growth by modifying the growth duration as a time series between 1 and 5 hours at the optimal temperature of 110 °C to enhance the PEC performance. The orientation and crystalline structure of ZnO NRs prepared at 110 °C between 1 to 5 hours was examined through X-ray diffraction. The detection of strong and sharp peak (002) indicated the aligned ZnO NRs were fabricated along *c-axis* of hexagonal wurtzite structure and perpendicular to ITO substrate in all resultant samples (Figure 8). The obtained results revealed that the intensity of the dominant sharp and strong peak of ZnO NRs (002) was significantly enhanced by increasing the growth time from 1 hour to 4 hours indicating an improvement in ZnO NRs crystalline properties. The average crystal size was boosted to 30.07 nm and 29.55 nm when the growth time extended for 4 and 5 hours, respectively; although, there were no remarkable changes in the averages of crystal size ZnO NRs for 1, 2 and 3 hours ( $\approx 25.07$ nm).

The intensity of the dominant peak (002) increased by increasing the growth duration from 1 to 4 hours and then declined with further prolonged growth period. The highest diffraction peak intensity, small FWHM of diffraction peak (002) was observed in the aligned ZnO NRs grown for 4 hours, which implies the suitability of this condition to provide high crystalline quality of ZnO NRs.

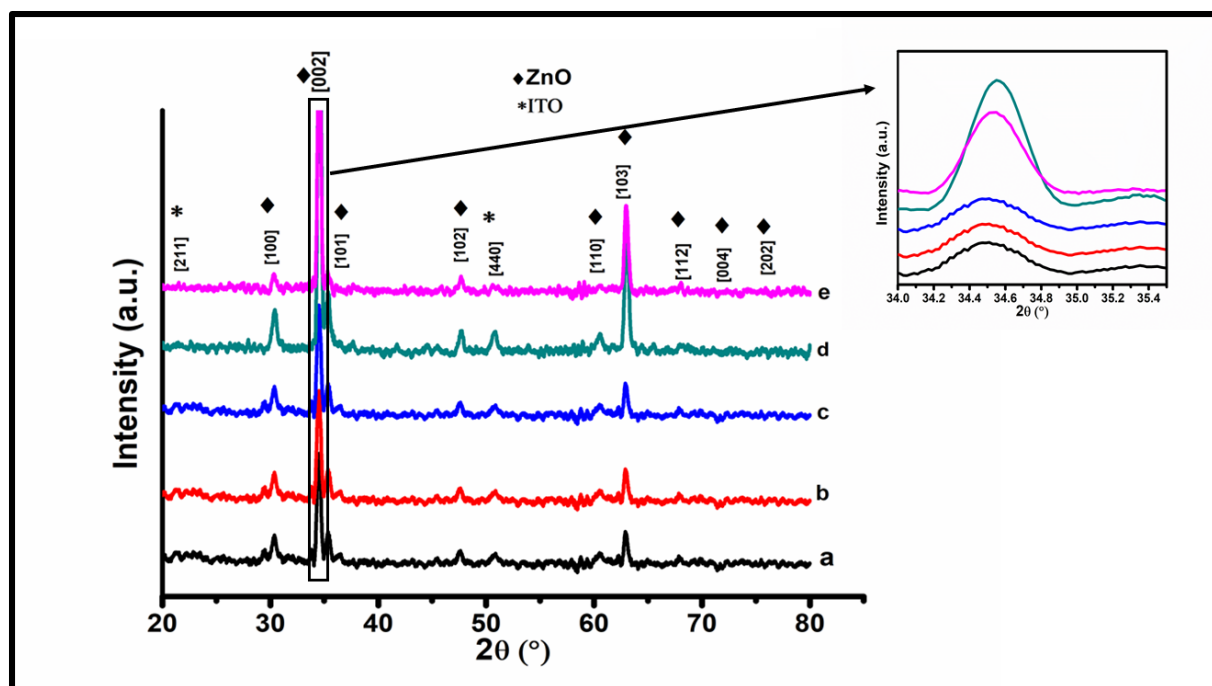
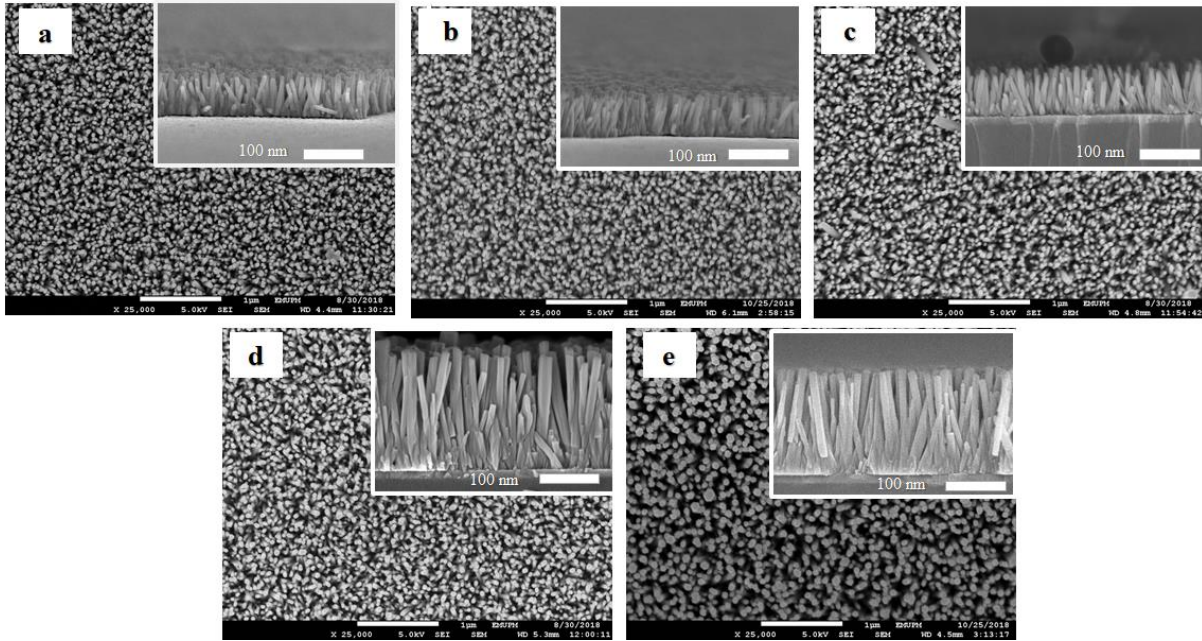


**Figure 8.** X-ray diffractograms of ZnO NRs prepared at 110 °C using hydrothermal method at different growth time: (a) 1h;(b) 2h; (c) 3h; (d) 4h; and (e) 5h. The inset of Figure 8 represents the (002) peak plotted from 34° to 35.5°.

The surface and cross-section images of the aligned ZnO NRs fabricated at 110 °C as a function of growth duration ranging between 1 and 5 hours is presented in Figure 9. The length of ZnO NRs increased dramatically achieving the highest aspect ratio (20.45) at 4 hours before showing decrement at 5 hours (Table 3). The diameters of all samples were found with average around 35 nm; although, the length of ZnO NRs increased significantly from 1 to 4 hours. This finding can be explained through the low concentration of  $Zn^{2+}$  and  $OH^-$  in un-refreshed growth solution of hydrothermal process based on the mechanism of ZnO NRs growth. Moreover, increased growth time might result in the dissolution of ZnO NRs from the reversed reaction (Equation 5).

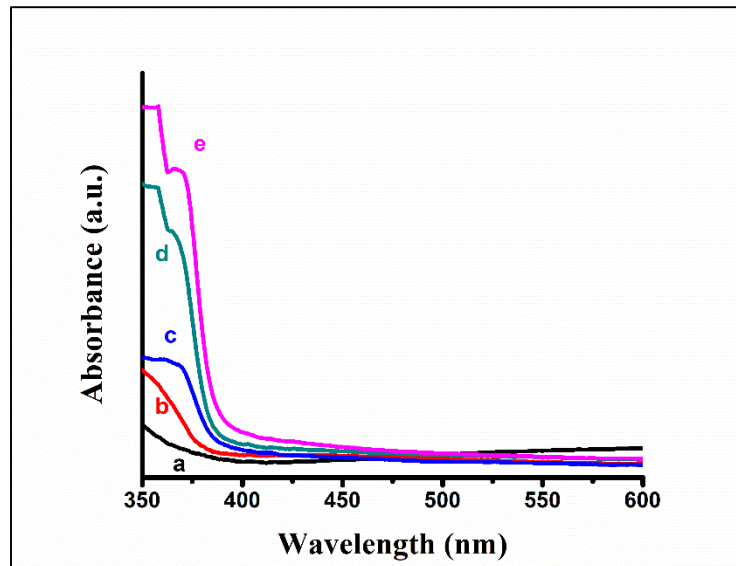
**Table 3** Summarized data from FE-SEM images of ZnO/ITO NRs at 110 °C for different growth time

Growth time (hour)	Length (nm)	Diameter (nm)	Aspect ratio
1	288.02	36.53	07.88
2	327.48	29.09	11.26
3	367.64	30.99	11.86
4	758.59	37.10	20.45
5	529.82	36.08	14.68



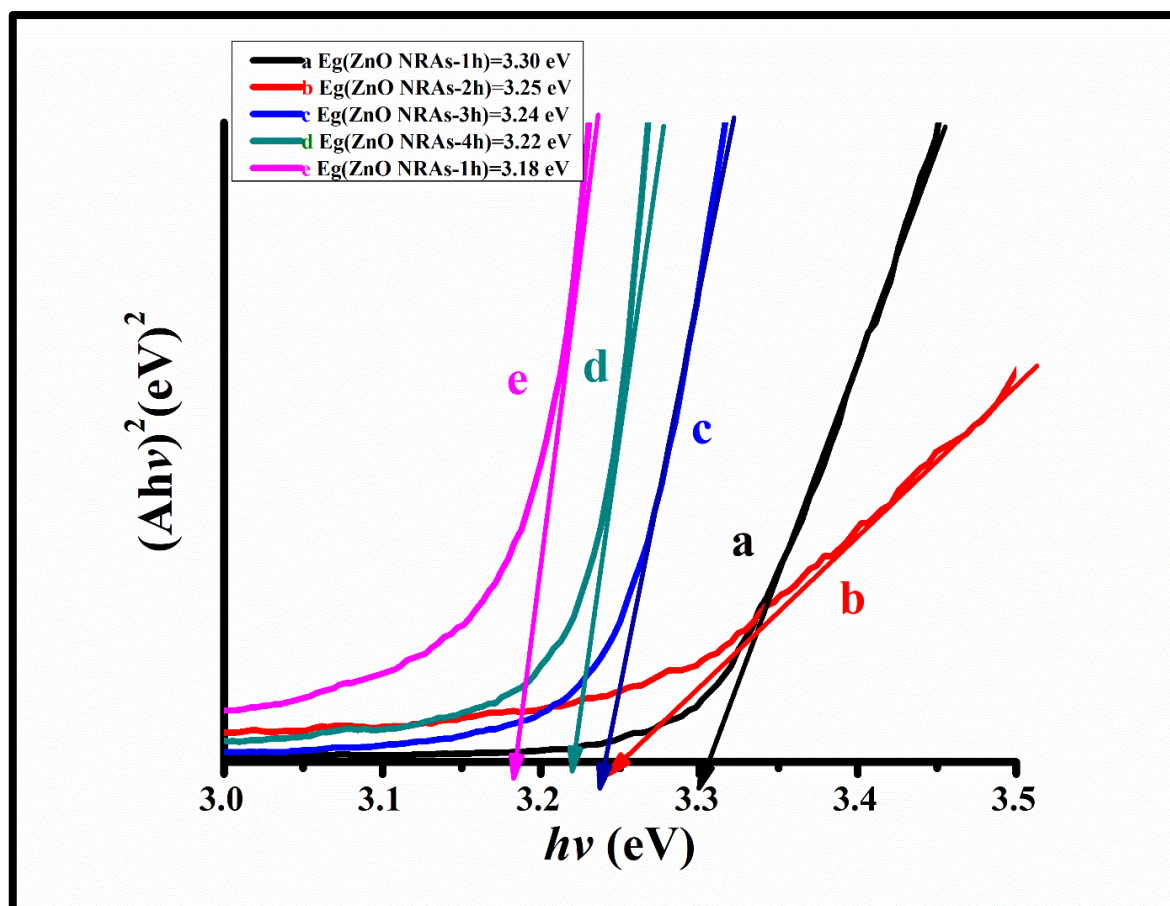
**Figure 9.** Top view and cross section FE-SEM images of ZnO NRs/ITO grown at 110 °C for different growth time: (a) 1h; (b) 2h; (c) 3h; (d) 4h; and (e) 5h.

Figure 10 displays the absorbance spectra of ZnO NRs prepared at 110 °C via the hydrothermal method at different hydrothermal growth between 1 and 5 hours. It can be observed that the increasing growth time caused a red-shift. The absorbance edges were 375.80, 381.53, 382.72, 385.09 and 389.90 nm at 1, 2, 3, 4 and 5 hours, respectively.



**Figure 10.** The absorbance spectra of ZnO NRs/ITO grown at 110°C via hydrothermal method for different hydrothermal method at different growth time: (a) 1h; (b) 2h; (c) 3h; (d) 4h; and (e) 5h.

Figure 11 plotted values for optical band gap energy of ZnO NRs prepared at 110 °C as a function of growth time. The optical band gap energy of ZnO NRs as a function of growth time of 1, 2, 3, 4, and 5 hours were 3.30, 3.25, 3.24, 3.22, 3.18 eV, respectively. The results depict good agreement with study reported by Abdulrahman et al. [26]. Significant improvement in crystal properties of ZnO NRs resulted in decreased optical band gap energy due to the increase in growth time (Figure 12).



**Figure 11.** The Tauc plot  $(\alpha hv)^2$  versus energy  $(hv)$  ZnO NRs/ITO grown at 110°C via hydrothermal method at different growth time: (a) 1h;(b) 2h; (c) 3h; (d) 4h; and (e) 5h.

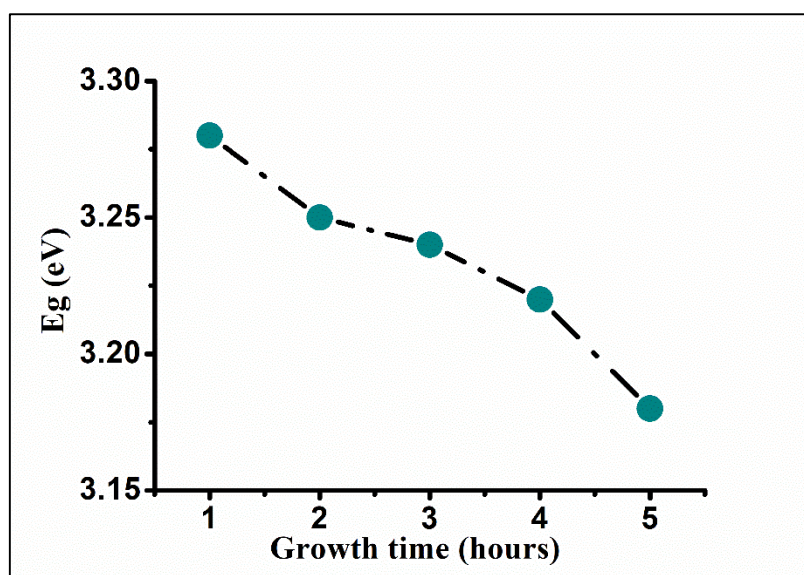


**Figure 12.** Graph of optical band gap energy of ZnO NRs prepared via hydrothermal method at 110 °C against the growth duration.

Linear sweep voltammetry (LSV) technique was used to evaluate the photoelectrochemical performance of ZnO NRs that prepared at 110 °C as a function of growth time in the ranging 1

and 5 hours (Figure 13). From this Figure, it can be observed that there was an enhancement in PEC performance when the growth time increased from 1 hour to 4 hours before showing decrement when the growth time extended to 5 hours. It is believed that the OH<sup>-</sup> might continuously hydrolyse in the water solution from HMTA up to 4 hours. Then, OH<sup>-</sup> would be consumed, so the surface area of ZnO NRs decreased as proven by the findings of FE-SEM and X-ray diffraction. In a closed system, the quantity of precursor ions was limited since the growth solution did not refresh during the hydrothermal process. The growth of ZnO NRs to form elongated continuously required more Zn<sup>2+</sup> leading to inhalation of the growth process. Consequently, the aspect ratio decreased, which affected the photocurrent density. This results in a good agreement with the previous studies [17, 20, 26].

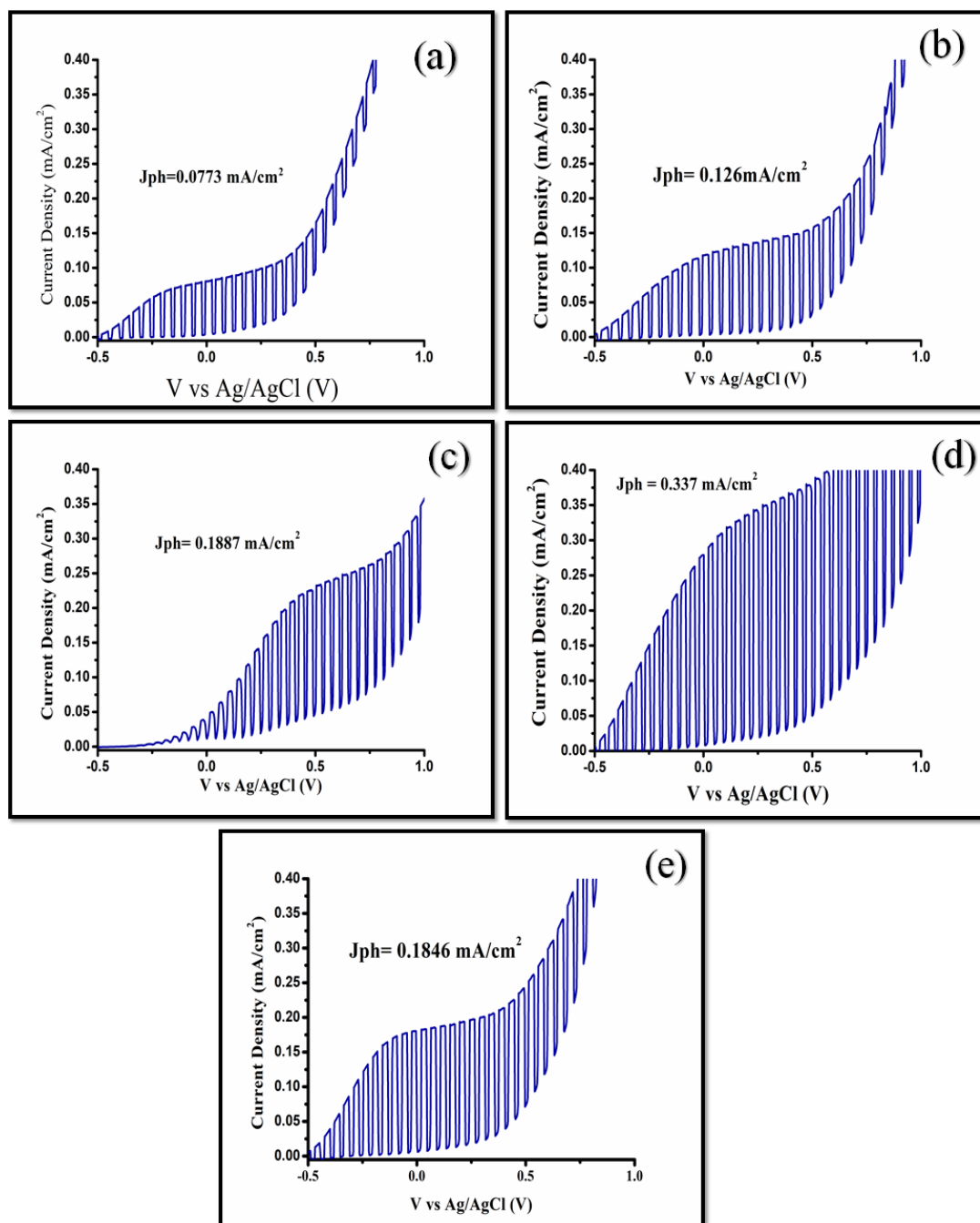


**Figure 13.** Linear sweep voltammograms of ZnO NRs/ITO synthesized at 110 °C using hydrothermal method at different growth time: (a) 1h; (b) 2h; (c) 3h; (d) 4h; and (e) 5h.

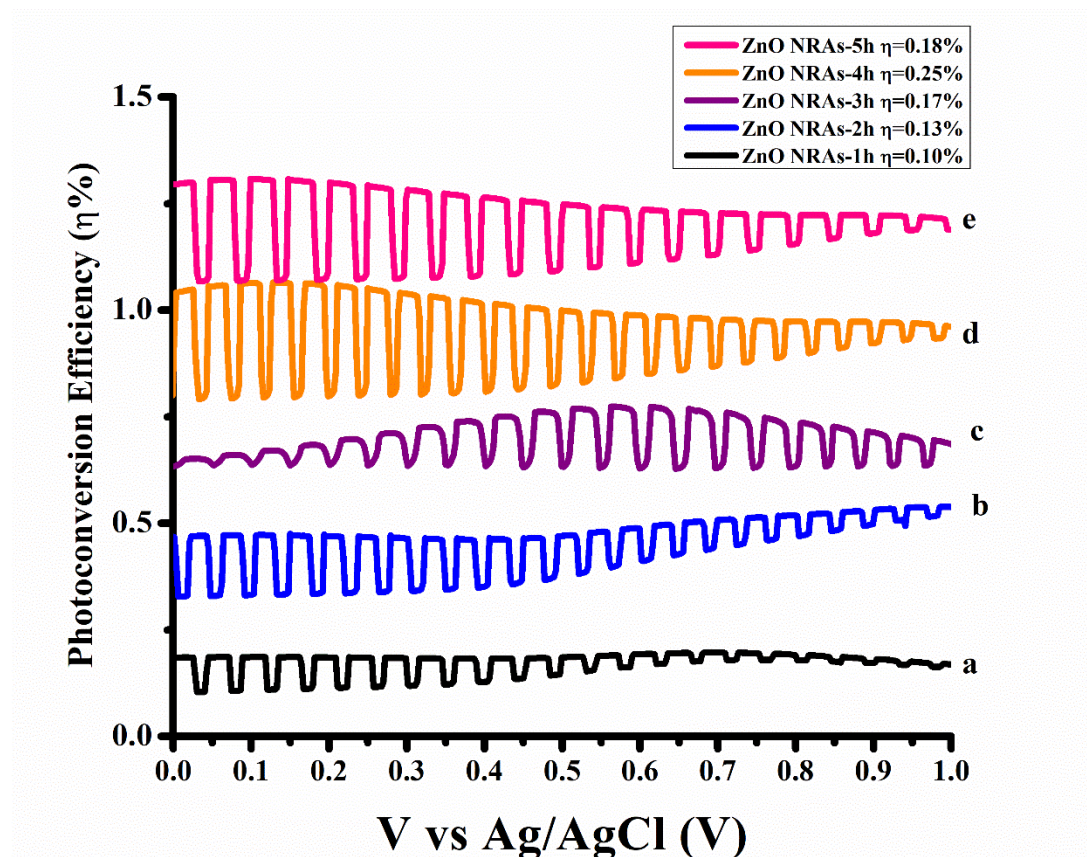


**Figure 14.** Photo conversion efficiency values ZnO NRs/ITO synthesized at 110 °C using hydrothermal method at different growth time: (a) 1h; (b) 2h; (c) 3h; (d) 4h; and (e) 5h under illumination intensity of 100 mWcm<sup>-2</sup> in 0.1M Na<sub>2</sub>S and 0.1M Na<sub>2</sub>SO<sub>3</sub> electrolyte system.

The values of photocurrent density  $J_{ph}$  were 0.0764, 0.1260, 0.1888, 0.337, and 0.1846 mA/cm<sup>2</sup> at 1, 2, 3, 4 and 5 hours respectively, which means the photocurrent density depends strongly on the growth duration (Figure 13). The enhancement of photocurrent density with increasing growth duration is a direct consequence of increasing the thickness of ZnO NRs, which improved light harvesting due to the efficient light absorption. It also facilitated the transportation of generated photoelectron and efficient diffusion of the holes to the redox species within the electrolyte that minimized recombination losses [33].

The reduction of  $J_{ph}$  at 5 hours may be due to the obtained decrement in surface area of ZnO NRs, as it is consistent with x-ray results. On the other hand, this study has reached the impressive photocurrent density of ZnO NRs fabricated at 110 °C for 4 hours (0.337 mA/cm<sup>2</sup>). It implied that the construction ZnO NRs under this condition would offer an effective direct transport pathway for the photogenerated electron that can abridge the distance of electron diffusion. Figure 14 shows the contribution towards impressive photoconversion efficiency (≈0.25). These results disclose that the large aspect ratio is an important key factor for the high photoconversion efficiency of ZnO NRs, which is in a good agreement with the observation of the FE-EM images. Table 4 displays the comparison between photocurrent densities and different ZnO NRs photoanodes that explains some of the PEC performance data.

**Table 4** Comparative study for synthesized ZnO NRs /ITO arrays at different hydrothermal growth temperature and growth time from different seed layers preparation methods

Sample	Seed layer synthesis method	Hydrothermal temperature (°C)	Hydrothermal growth time (hours)	J <sub>ph</sub> mAcm <sup>-2</sup>	Ref.
ZnO NRs/ITO	Spin coating	90	4	0.37 at 0.0 V vs Ag/AgCl	[20]
ZnO NRs/ITO	Spin coating	110	4	0.337 at +0.5 vs Ag/AgCl	Current study
ZnO NRs/ITO	Dip coating	120	4	0.194 at +0.5 V vs Ag/AgCl	[17]
ZnO NRs/FTO	Seed-layer mediated hydrothermal	150	12	0.50 at 1.23 V vs RHE	[33]
ZnO NRs/Zn foil	Modified hydrothermal method	180	5	0.33 at +0.1 V vs Ag/AgCl	[34]

#### 4. CONCLUSION

The study has shown the successful fabrication of high aspect ratio of well-aligned ZnO NRs array through a simple low-temperature hydrothermal process. The growth temperature and time-dependent growth control the morphological and structural characteristics of the grown samples obtain the desired ZnO NRs. The enlarged surface area of ZnO NRs for growth duration equal 4 hours made these experiments reproducible with impressive photo conversion efficiency ( $\approx 0.25\%$ ) for ZnO NRs prepared at 110 °C. Consequently, the transportation of the photogenerated electron improved dramatically, which reflected the PEC performance positively. A correlation between the growth time and morphological structure of ZnO NRs was observed by FE-SEM. The increasing consumption of hydrothermal growth ions namely Zn<sup>2+</sup> and OH<sup>-</sup> at 120 °C and 5 hours have affected negatively on the aspect ratio of ZnO NRs resulting deterioration of the photocurrent density of PEC.

#### REFERENCES

- [1] Regonini, D., Teloeken, A.C., Alves, A.K., Berutti, F.A., Gajda-Schranz, K., Bergmann, C.P., *et al.* Electrospun TiO<sub>2</sub> Fiber Composite Photoelectrodes for Water Splitting. *American Chemical Society (ACS)*. **5**, 22 (2013) 11747–11755.
- [2] Ingler, W. B., Khan, S. U. M. A Self-Driven p/n-Fe[sub2]O[sub3] Tandem Photoelectrochemical Cell for Water Splitting. *The Electrochemical Society*. **9**, 4 (2006) G144.
- [3] Eswar, K. A., Husairi, F. S., Ab Aziz, A., Rusop, M., Abdullah, S. Effect of Post Annealing Temperature on Surface Morphology and Photoluminescence Properties of ZnO Thin Film. *Trans Tech Publications*. **832** (2013) 654–658.
- [4] Kuo, S-Y., Chen, W-C., Lai, F-I., Cheng, C-P., Kuo, H-C., Wang, S-C., *et al.* Effects of doping concentration and annealing temperature on properties of highly-oriented Al-doped ZnO films. *Elsevier BV*. **287**, 1 (2006) 78–84.
- [5] Venu Gopal, V. R., Kamila, S. Effect of temperature on the morphology of ZnO nanoparticles: a comparative study. *Applied Nanoscience*. **7**, 3-4 (2017) 75–82.
- [6] Kong, Y., Sun, H., Fan, W., Wang, L., Zhao, H., Zhao, X., *et al.* Enhanced photoelectrochemical performance of tungsten oxide film by bifunctional Au nanoparticles. *RSC Advances*. **7**, 25 (2017) 15201–15210.

- [7] Miao, J., Liu, B. II-VI semiconductor nanowires. *Semiconductor Nanowires*, (2015) 3–28.
- [8] Rattanawarinchai, P., Khemasiri, N., Jessadaluk, S., Chananonnawathorn, C., Horprathum, M., Klamchuen, A., *et al.* Growth time dependence on photoelectrochemical property of zinc oxide nanorods prepared by hydrothermal synthesis. *World Scientific Pub Co Pte Lt*, (2018), 1840001.
- [9] Kim, D., Leem, J-Y. Effect of the pH of an Aqueous Solution on the Structural, Optical, and Photoresponse Properties of Hydrothermally Grown ZnO Nanorods and the Fabrication of a High Performance Ultraviolet Sensor. *Journal of the Korean Physical Society*. **72**, 3 (2018) 400–405.
- [10] Ohyama, M., Kouzuka, H., Yoko, T. Sol-gel preparation of ZnO films with extremely preferred orientation along (002) plane from zinc acetate solution. *Thin Solid Films*. **306**, 1 (1997) 78–85.
- [11] Mah, C. F., Yam, F. K., Hassan, Z. Investigation and Characterization of ZnO Nanostructures Synthesized by Electrochemical Deposition. *Procedia Chemistry*. **19** (2016) 83–90.
- [12] Thongsuksai, W., Panomsuwan, G., Rodchanarowan, A. Fast and convenient growth of vertically aligned ZnO nanorods via microwave plasma-assisted thermal evaporation. *Materials Letters*. **224** (2018) 50–53.
- [13] Murkute, P., Ghadi, H., Saha, S., Pandey, S.K., Chakrabarti, S. Enhancement in optical characteristics of c-axis-oriented radio frequency-sputtered ZnO thin films through growth ambient and annealing temperature optimization. *Materials Science in Semiconductor Processing*. **66** (2017) 1–8.
- [14] Husna J, Aliyu MM, Islam MA, Chelvanathan P, Hamzah NR, Hossain MS, Karim MR, Amin N. Influence of annealing temperature on the properties of ZnO thin films grown by sputtering. *Energy Procedia*. **25** (2012) 55-61.
- [15] Meng, F., Ge, F., Chen, Y., Xu, G., Huang, F. Local structural changes induced by ion bombardment in magnetron sputtered ZnO: Al films: Raman, XPS, and XAS study. *Surface and Coatings Technology*, (2018).
- [16] Nasirpouri, F. *Electrodeposition of Nanostructured Materials*. Springer Series in Surface Sciences, (2017).
- [17] Mohd Fudzi, L., Zainal, Z., Lim, H., Chang, S-K., Holi, A., Sarif Mohd, A. M. Effect of Temperature and Growth Time on Vertically Aligned ZnO Nanorods by Simplified Hydrothermal Technique for Photoelectrochemical Cells. *Materials*. **11**, 5 (2018) 704.
- [18] Worasawat, S., Masuzawa, T., Hatanaka, Y., Neo, Y., Mimura, H., Pecharapa, W. Synthesis and characterization of ZnO nanorods by hydrothermal method. *Materials Today: Proceedings*. **5**, 5 (2018) 10964–10969.
- [19] Wang, C., Zhang, X., Wang, D., Yang, Z., Ji, W., Zhang, C., *et al.* Synthesis of nanostructural ZnO using hydrothermal method for dye-sensitized solar cells. *Science China Technological Sciences*. **53**, 4 (2010) 1146–1149.
- [20] Holi, A.M., Zainal, Z., Talib, Z.A., Lim, H-N., Yap, C-C., Chang, S-K., *et al.* Effect of hydrothermal growth time on ZnO nanorod arrays photoelectrode performance. *Optik*. **127**, 23 (2016) 11111–11118.
- [21] Murillo, G., Lozano, H., Cases-Utrera, J., Lee, M., Esteve, J. Improving Morphological Quality and Uniformity of Hydrothermally Grown ZnO Nanowires by Surface Activation of Catalyst Layer. *Nanoscale Research Letters*. **12**, 1 (2017).
- [22] Rana, A., ul, H.S., Chang, S-B., Chae, H.U., Kim, H-S. Structural, optical, electrical, and morphological properties of different concentration sol-gel ZnO seeds and consanguineous ZnO nanostructured growth dependence on seeds. *Journal of Alloys and Compounds*. **729** (2017) 571–582.
- [23] Choi, H-S., Vaseem, M., Kim, S.G., Im, Y-H., Hahn, Y-B. Growth of high aspect ratio ZnO nanorods by solution process: Effect of polyethyleneimine. *Journal of Solid-State Chemistry*. **189** (2012) 25–31.
- [24] Murillo, G., Lozano, H., Cases-Utrera, J., Lee, M., Esteve, J. Improving Morphological Quality and Uniformity of Hydrothermally Grown ZnO Nanowires by Surface Activation of Catalyst Layer. *Nanoscale Research Letters*. **12**, 1(2017).

- [25] Gautam, K., Singh, I., Bhatnagar, P. K., Peta, K. R. The effect of growth temperature of seed layer on the structural and optical properties of ZnO nanorods. *Superlattices and Microstructures*. **93** (2016) 101–108.
- [26] Abdulrahman, A. F., Ahmed, S. M., Almessiere, M. A. Effect of The Growth Time on The Optical Properties of ZnO Nanorods Grown by Low Temperature Method. *Digest Journal of Nanomaterials & Biostructures (DJNB)*. **12** (2017).
- [27] Kandel, E. R., Tauc, L. Anomalous rectification in the metacerebral giant cells and its consequences for synaptic transmission. *The Journal of physiology*. **183** (1966) 287-304.
- [28] Rodnyi, P. A., Khodyuk, I.V. Optical and luminescence properties of zinc oxide (Review). *Optics and Spectroscopy*. **111**, 5 (2011) 776–785.
- [29] Janotti, A., Van de Walle, C.G. Fundamentals of zinc oxide as a semiconductor. *Reports on Progress in Physics*. **72**, 12 (2009), 126501.
- [30] Narayanan, G. N., Sankar, Ganesh, R., Karthigeyan, A. Effect of annealing temperature on structural, optical and electrical properties of hydrothermal assisted zinc oxide nanorods. *Thin Solid Films*. **598** (2016) 39–45.
- [31] Sanjeev, S., Kekuda, D. Effect of Annealing Temperature on the Structural and Optical Properties of Zinc Oxide (ZnO) Thin Films Prepared by Spin Coating Process. *IOP Conference Series: Materials Science and Engineering*. **73** (2015) 012149.
- [32] Shrisha, B. V., Bhat, S., Kushavah, D., Gopalakrishna, Naik, K. Hydrothermal growth and characterization of Al-doped ZnO nanorods. *Materials Today: Proceedings*. **3**, 6 (2016) 1693–1701.
- [33] Lou, Y-Y., Yuan, S., Zhao, Y., Wang, Z-Y., Shi, L-Y. Influence of defect density on the ZnO nanostructures of dye-sensitized solar cells. *Advances in Manufacturing*. **1**, 4 (2013) 340–345.
- [34] Hou, T-F., Boppella, R., Shanmugasundaram, A., Kim, D.H., Lee, D-W. Hierarchically self-assembled ZnO architectures: Establishing light trapping networks for effective photoelectrochemical water splitting. *International Journal of Hydrogen Energy*. **42**, 22 (2017) 15126–15139.

